

# Monte Carlo Analysis of the Behavior and Spatial Origin of Electronic Noise in GaAs MESFET's

Tomás González, Daniel Pardo, Luca Varani, and Lino Reggiani

**Abstract**—We present a Monte Carlo (MC) analysis of electronic noise associated with velocity and field fluctuations in GaAs MESFET's. To this end, an accurate estimator of the instantaneous currents at the terminals is used, which improves the precision of the method. Both the current and voltage fluctuations at the different terminals of the device are investigated, thus allowing for the spatial localization of the noise sources. Three different MESFET geometries are analyzed. The results so found compares well with experimental results and confirm the general trend provided by existing phenomenological noise modeling. As a general result, the noise in the drain current is found to increase with the level of the current and remain constant with frequency at least up to 100 GHz. In the case of the gate current, the noise is null at low frequency and then increases quadratically. Under saturation conditions, the source of the drain-voltage fluctuations is localized at the drain end of the  $n$  channel, and even penetrates the drain  $n^+$  region due to the presence of hot carriers in the upper valleys.

## I. INTRODUCTION

THE widespread use of GaAs MESFET's for low-noise high-frequency applications makes necessary a detailed characterization of the noise performances in these devices [1]. The improvements achieved by the fabrication technologies must be accompanied by the development of theories able to explain the physical background of the microscopic noise sources. The methods usually employed to this end need to introduce approximations related to the statistical properties of the noise sources [2], generally by characterizing the velocity fluctuations at a given position through the diffusion coefficient of the bulk material corresponding to the local electric field [3], [4]. As an alternative to these models, the Monte Carlo (MC) method has the advantage that the sources of diffusion noise as well as the fluctuating fields are naturally accounted for in the simulation, which provides directly their behavior. Therefore, it is not necessary to incorporate them externally. Moreover, the MC simulation includes all the processes relevant to the transport in small semiconductor devices (nonstationary effects, hot carriers, etc.).

The MC method has already been employed successfully to investigate the properties of noise in semiconductor materials

and one-dimensional devices (resistors,  $n^+nn^+$  structures, Schottky-barrier diodes, etc.) [5]–[8]. However, in the case of MESFET's (and three-terminal devices in general), while widely used for the study of the static characteristics [9]–[11], it has been scarcely applied to analyze noise characteristics [12]. The main difficulty involved in this analysis is to have a good estimator of the currents at the terminals in order to extract the information relevant to noise. To this purpose, the approach which is usually employed consists, for the conduction current, in counting the net number of particles crossing the terminals at each time step and, for the displacement current, in making the time derivative of the field at the contacts [13]. This approach, which is appropriate to obtain average stationary values, is not sufficiently accurate to study fluctuations. In this paper we make use of a recent technique proposed by Gruzinskis *et al.* [14] which makes possible an improvement in the accuracy of the calculations to the extent of analyzing the intrinsic noise of the device [15].

By applying two complementary operation modes, we present a two-dimensional MC analysis of the current and voltage fluctuations at the gate and drain terminals of GaAs MESFET's. In addition, we provide the spatial location of the voltage noise inside the device. Three different MESFET geometries and their influence on the noise performance are considered; and only the noise processes related to the intrinsic behavior of the device are investigated. The paper is organized as follows. In Section II, the details of the physical model, concerning the MC particle simulation and the MESFET geometries considered, are described. In Section III, the theoretical basis and the applied operation modes are presented. The results of the simulations are given and discussed in Section IV. Finally, the main conclusions are summarized in Section V.

## II. PHYSICAL MODEL

### A. Simulated MESFET's

The noise analysis is carried out mostly for the structure shown in Fig. 1(a) (MESFET A). It consists of an  $n^+nn^+$  structure with a one-micron channel modulated by a gate contact of 0.5  $\mu\text{m}$ . The source and drain contacts are placed at the end of the  $n^+$  regions and are 0.2  $\mu\text{m}$  long. Two slight modifications of this geometry are then introduced in order to analyze their influence on the MESFET noise performance. Firstly, a GaAs semi-insulating substrate is included, like shown in Fig. 1(b) (MESFET B). Secondly, starting from

Manuscript received June 16, 1994; revised December 21, 1994. The review of this paper was arranged by Associate Editor J. R. Hauser.

T. González and D. Pardo are with the Departamento de Física Aplicada, Universidad de Salamanca, 37008 Salamanca, Spain.

L. Varani is with the Centre d'Electronique de Montpellier, Université Montpellier II, 34095 Montpellier Cedex 5, France. He is on leave from the Dipartimento di Fisica, Università di Modena, 41100 Modena, Italy.

L. Reggiani is with the Dipartimento di Fisica ed Istituto Nazionale di Fisica della Materia, Università di Modena, 41100 Modena, Italy.

IEEE Log Number 9410479.

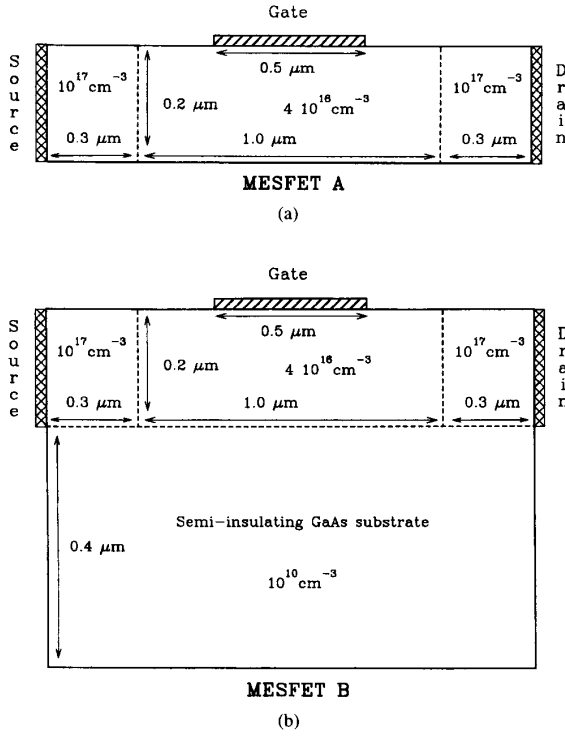


Fig. 1. Cross section of the MESFET geometries considered: (a) MESFET A, without substrate, (b) MESFET B, with substrate.

MESFET B, the gate is displaced  $0.1 \mu\text{m}$  toward the source (MESFET C, not shown in Fig. 1).

The doping level of the source and drain regions is set to  $10^{17} \text{ cm}^{-3}$ , far from the values used in real MESFET's (around  $10^{18} \text{ cm}^{-3}$ ), in order to get affordable computation times in the simulations. When calculating magnitudes related to the noise (correlation functions), the simulated time must be considerably increased (by a factor around 100) with respect to the case of calculating static characteristics. Increasing the doping level to  $10^{18} \text{ cm}^{-3}$  in the  $n^+$  regions would multiply the computation time by a factor higher than 10, leading to too long CPU times. The noise behavior obtained for low dopings can be initially extrapolated to higher values, since the physical model would be basically the same. However, some changes can be expected. The elements which could modify the observed electronic noise would be the higher efficiency of impurity scattering (which in principle reduces the noise) and the presence of electron-electron scattering and Pauli exclusion principle (whose influence on the noise is a subject to be studied).

The positioning of the contacts at the sides of the structures instead of the common planar geometry is due to two reasons. Firstly, it makes practicable the implementation of the algorithms used for the noise analysis and reduces considerably the uncertainty of the calculations due to the time discretization of the equations, as will be seen in the following section. Secondly, it allows for a direct comparison of the results obtained for MESFET A with those obtained

from the one-dimensional simulation of the  $n^+nn^+$  structure corresponding to MESFET A without gate. In any case, the MESFET noise properties are expected to be not significantly affected by the positioning of the contacts.

### B. Monte Carlo Simulation

The simulation of the GaAs MESFET's is performed by coupling self-consistently a two-dimensional Poisson's solver with an ensemble MC simulator, which is three dimensional in momentum space and two dimensional in real space. The MC procedure follows the standard scheme [16]. The value adopted for the nonsimulated dimension of the devices is  $0.714 \mu\text{m}$ , which means an average number of simulated carriers between 9500 and 13000 depending on the bias. The model for the GaAs conduction band consists of three nonparabolic spherical valleys ( $\Gamma$ ,  $L$  and  $X$ ). The scattering mechanisms and the GaAs physical parameters employed in the simulation are the same as those used for the valleys of the first conduction band in previous works [17]. To solve Poisson's equation, a uniform grid formed of  $160 \times 25$  meshes of  $100 \times 80 \text{ \AA}$  is used for MESFET A, and a nonuniform grid of  $160 \times 44$  meshes for MESFET's B and C. The electric field is updated with a time step of 10 fs for the current-noise calculations, and of 2.5 fs for the voltage-noise calculations. The simulation is performed at 300 K.

## III. THEORETICAL ANALYSIS

### A. Current Calculation

The prerequisite of the present noise analysis is to obtain accurate values of the instantaneous currents at the terminals, including the displacement contribution. To this end, here we make use of the technique proposed in [14]. For the geometry of MESFET A (see Fig. 1(a)), and assuming the source contact as reference ( $V_S = 0$ ), the currents per unit length at the source, drain and gate at a time  $t$ ,  $I_s(t)$ ,  $I_d(t)$  and  $I_g(t)$ , are given by:

$$I_s(t) = \frac{1}{x_{g1}} \left\{ Q \sum_i^{0-x_{g1}} v_{xi}(t) - \frac{\epsilon_0 \epsilon_r}{\Delta t} \sum_{j=1}^{M_y} \Delta y_j \cdot [\varphi(x_{g1}, y_j, t) - \varphi(x_{g1}, y_j, t - \Delta t)] \right\} \quad (1)$$

$$I_d(t) = \frac{1}{x_d - x_{g2}} \left\{ Q \sum_i^{x_{g2}-x_d} v_{xi}(t) + \frac{\epsilon_0 \epsilon_r}{\Delta t} \sum_{j=1}^{M_y} \Delta y_j \cdot [\varphi(x_{g2}, y_j, t) - \varphi(x_{g2}, y_j, t - \Delta t)] - \frac{\epsilon_0 \epsilon_r h}{\Delta t} [V_D(t) - V_D(t - \Delta t)] \right\} \quad (2)$$

$$I_g(t) = I_s(t) - I_d(t) \quad (3)$$

where  $\epsilon_0 \epsilon_r$  is the dielectric constant of the material,  $\Delta t$  the time step,  $Q$  the linear charge density of a particle,  $v_{xi}$  the velocity in the  $x$  direction of the  $i$ th particle,  $M_y$  the number of vertical meshes,  $\Delta y_j$  the vertical dimension of the  $j$ th vertical

mesh,  $y_j$  its  $y$  position,  $\varphi$  the electric potential,  $h$  the vertical dimension of the device,  $V_D$  the drain voltage, and  $x_{g1}$ ,  $x_{g2}$ , and  $x_d$  the  $x$  positions respectively of the left edge of the gate, the right edge of the gate, and the drain. The summation over  $i$  is performed over the particles with  $x$  position between 0 and  $x_{g1}$  in the case of the source current, and between  $x_{g2}$  and  $x_d$  in the case of the drain current. Similar expressions apply to the case of MESFET's B and C, which consider the fact that the source and drain contacts do not extend along the whole sides of the structures.

If the contacts were placed at the top of the structures, then (1) and (2) would contain the time derivative of the potential in a second column of meshes and  $V_D$  would not appear explicitly in the equations [14]. This would mean that the mathematical uncertainty introduced by the time discretization would increase considerably, and that the second of the operation modes described in the following would be much more difficult to implement.

### B. Operation Modes

From a general point of view, a noisy MESFET (or any two-port device) can be represented by the noiseless MESFET together with two correlated noise sources. Therefore, apart from the behavior of the noiseless device, four parameters are needed for the full noise description of the MESFET: the spectral density of two noise sources and their complex correlation coefficient [1]. Several equivalent representations can be used to this purpose, with either current or voltage noise sources, so that a simple transform formula can be found to pass from one representation to the other [18]. The characterization of the noiseless device is made by the determination of the MESFET small-signal equivalent circuit, which can also be easily done by means of the MC simulation, as shown in [19]. Here we shall focus on the calculation of the noise sources.

In this work, the noise in the MESFET is analyzed by employing two of the above-mentioned representations, which we shall call current- and voltage-noise operation modes, respectively. In both modes the fluctuations are analyzed through the calculation of the respective autocorrelation and cross-correlation functions, which, after Fourier transform, give the spectral densities. To provide an adequate resolution of these functions, the carrier kinetics inside the device is simulated under stationary conditions during 650 ps, which is a time long enough to get smooth results (and convergence) both for the correlation functions and spectral densities. It must be stressed that the analysis performed with the MC method is only related to the intrinsic noise of the device, thus disregarding any external noise sources (like those associated with the contacts) or parasitic effects.

1) *Current-Noise Operation*: In this mode, the gate and drain voltages remain constant in time, and the fluctuations of the short-circuit currents and their correlation are investigated. The current-noise sources are represented as two (correlated) current generators in parallel at the input and output of the MESFET, as shown in Fig. 2(a). Since  $V_D$  is constant, in this operation mode the last two terms in (2) cancel each other.

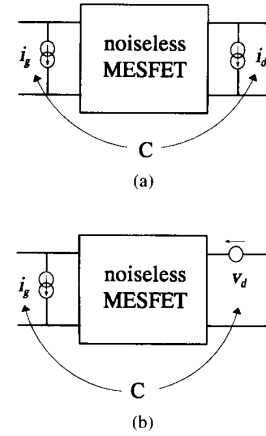


Fig. 2. Representations of the noisy MESFET corresponding to the two-operation modes in which the noise is analyzed: (a) current-noise operation; (b) voltage-noise operation.

2) *Voltage-Noise Operation*: In this mode, the gate voltage and the drain current remain constant in time, and the fluctuations of the short-circuit gate current, of the open-circuit drain voltage and their correlation are investigated. The noise sources are represented as a current generator in parallel at the input and a voltage generator in series at the output (correlated with the current generator), as shown in Fig. 2(b). If we consider that the drain current is constant and equal to  $I_{D0}$ , the instantaneous value of  $V_D$  at a time  $t$  is obtained from (2) as:

$$V_D(t) = V_D(t - \Delta t) - \frac{\Delta t}{\epsilon_0 \epsilon_r h} \cdot \left[ I_{D0}(x_d - x_{g2}) - Q \sum_i^{x_{g2}-x_d} \nu_{xi}(t) \right] + \frac{1}{h} \sum_{j=1}^{M_y} \Delta y_j [\varphi(x_{g2}, y_j, t) - \varphi(x_{g2}, y_j, t - \Delta t)] \quad (4)$$

which is calculated in the simulation by applying an iterative technique, since it is not possible to know the value of  $\varphi(x_{g2}, y, t)$  without knowing previously  $V_D(t)$ , which is used as boundary condition at the drain contact to obtain the potential. Thus, Poisson's equation is solved successively for three times at the end of each time step: the first one with the old value of  $V_D$  and the new carrier space-distribution, and the two following ones with the value of  $V_D$  updated through (4) by using the values of  $\varphi(x_{g2}, y, t)$  from the preceding solution. The last two estimations of  $V_D$  are practically the same, what confirms the convergence of the technique.

Since during the simulation we have the value of the potential at the grid points for each time step, with this operation mode we can perform a spatial analysis of the voltage fluctuations by calculating the voltage spectral density as a function of the position  $(x, y)$ , as already reported for the case of one-dimensional structures [6].

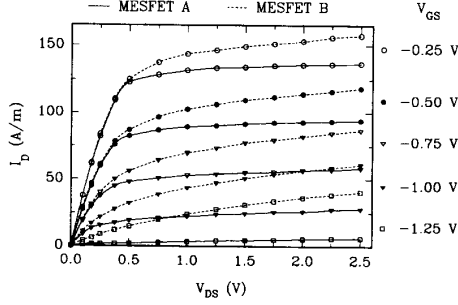


Fig. 3. Drain-current versus drain-voltage characteristics of MESFET's A and B. The current in MESFET C is practically the same as that of MESFET B. The gate voltages include the built-in potential of the Schottky contact ( $-0.7$  V).

#### IV. RESULTS AND DISCUSSION

Before reporting the results of the noise analysis, Fig. 3 shows the drain-current versus drain-voltage characteristics of MESFET's A and B. In the case of MESFET C the characteristics are practically the same as those obtained for MESFET B, apart from a slight increase of the current at the lowest values (in magnitude) of  $V_{GS}$ . The gate voltages include the built-in potential of the Schottky contact ( $-0.7$  V). The drain current, after a short linear dependence, exhibits a saturation region, which is due to the screening effect of the gate on the source region [10] and to the transfer of carriers to the upper valleys. The saturation is less pronounced in MESFET's B and C due to the flux of current through the substrate. To give an idea of the electrical performances of these devices, for the operating point  $V_{GS} = -0.25$  V,  $V_{DS} = 1.5$  V, the transconductance  $g_m$  and the current-gain cut-off frequency  $f_T$  are, respectively, 190 mS/mm and 47.5 GHz in MESFET A, and 177 mS/mm and 44.5 GHz in MESFET B.

##### A. Current-Noise Operation

Since currents are calculated per unit length, the current spectral densities are given in  $A^2sm^{-2}$ , and to convert their values for the case of a real device with the same cross-section, the results given here should be multiplied by the depth of the simulated MESFET ( $0.714 \mu m$ ) and by the depth of the real device, thus accounting for the scaling factor introduced by the different number of carriers considered. Fig. 4 shows the dependence on frequency we find for the spectral density of the short-circuit drain- and gate-current fluctuations,  $S_{i_D}$  and  $S_{i_G}$ , in the saturation region of MESFET A.  $S_{i_D}$  is practically constant with frequency, and increases proportionally with the value of the drain current. The noise at the gate is due to the capacitive coupling of the fluctuations in the potential (carrier) distribution along the channel.  $S_{i_G}$  exhibits a  $f^2$  behavior, with a proportionality factor which also increases with the drain-current. The results of the MC simulation for the values of  $S_{i_G}$  at zero frequency are very small, and can be considered to be null within the statistical uncertainty of this method. In order to get exactly the  $f^2$  dependence at low frequencies (up to 10 GHz), it is necessary to subtract  $S_{i_G}(0)$  from  $S_{i_G}(f)$ . The results given in Fig. 4 are calculated in this way. The behaviors found for  $S_{i_D}$  and  $S_{i_G}$  are well known from the literature

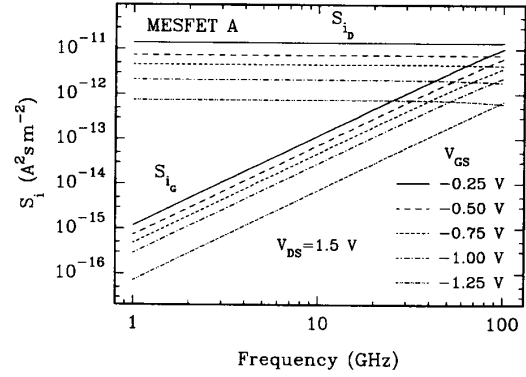


Fig. 4. Spectral density of short-circuit drain- and gate-current fluctuations as a function of frequency for several bias points in the saturation region of MESFET A corresponding to a drain voltage of 1.5 V.

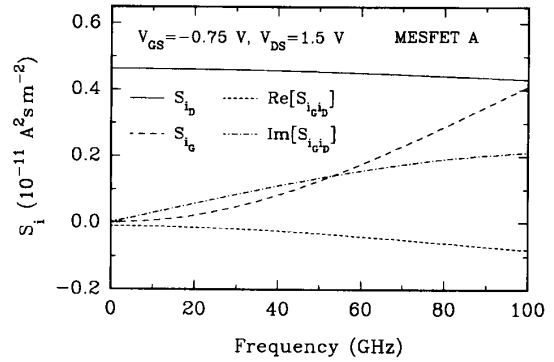


Fig. 5. Spectral density of short-circuit drain- and gate-current fluctuations, and real and imaginary parts of their cross correlation as a function of frequency for the operating point  $V_{GS} = -0.75$  V,  $V_{DS} = 1.5$  V in MESFET A.

[4], [20], [21]; but, to our knowledge, this is the first time which they are quantitatively obtained from a self-consistent MC simulation.

It must be emphasized that the resolution of the noise spectral densities estimated as the Fourier transform of the autocorrelation functions deteriorates specially when the values are small, like in the case of  $S_{i_G}$  at low-frequency. This is due to the long time tail of the autocorrelation functions (which do not vanish completely, but oscillate around zero) when integrated to calculate the Fourier transforms. Thus, the uncertainty in the results is high for the values of  $S_{i_G}$  at low frequency; for the rest of magnitudes (and for  $S_{i_G}$  at higher frequencies) the uncertainty is estimated to be within a  $\pm 15\%$ . To increase the accuracy, a higher number of carriers, a smaller grid size and a longer simulation time are needed; requirements which are not always affordable from the point of view of computation time. Other methods to estimate the spectral densities, like the one presented in [22], could improve the exactness, but always at the expense of a longer simulation time. In any case, the results obtained with the present technique are correct enough to characterize completely the noise behavior in the MESFET.

Fig. 5 shows the spectral density of the drain- and gate-current fluctuations and the real and imaginary parts of their

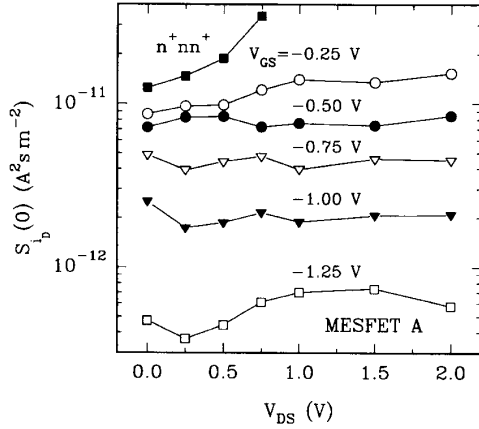


Fig. 6. Low-frequency value of the spectral density of short-circuit drain-current fluctuations as a function of the drain voltage for several gate voltages in MESFET A. The current spectral density in the  $n^+nn^+$  structure corresponding to MESFET A without gate is also included.

cross-correlation,  $S_{i_G i_D}$ , for the operating point  $V_{GS} = -0.75$  V,  $V_{DS} = 1.5$  V in MESFET A.  $S_{i_D}$  and  $S_{i_G}$  present the behavior already commented. The imaginary part of the cross-correlation increases proportionally with frequency, according to predictions [20], at least up to 40 GHz. The real part takes small negative values but, despite the large uncertainty in this magnitude, is not strictly null at low frequencies, contrary to what expected [4], [21]. These results give a correlation coefficient, defined as  $jC(f) = S_{i_G i_D}(f) / \sqrt{S_{i_G}(f) S_{i_D}(f)}$ , with an imaginary part practically constant with frequency and a real part taking low negative values (for frequencies higher than 10 GHz), in agreement with the theoretical predictions [20] and other numerical determinations [4].

Fig. 6 reports the low-frequency value of the drain-current spectral density in MESFET A as a function of  $V_{DS}$  for several  $V_{GS}$ , together with the current spectral density in the  $n^+nn^+$  structure corresponding to MESFET A without gate (up to voltages below the onset for Gunn oscillations). As the absolute value of  $V_{GS}$  increases, thus narrowing the width of the  $n$  channel, the device becomes more resistive and  $S_{i_D}$  smaller. In the case of the  $n^+nn^+$  structure, where the whole  $n$  region is a conducting channel,  $S_i$  is larger and increases significantly near the threshold voltage for the Gunn oscillations. On the contrary,  $S_{i_D}$  in the MESFET exhibits smooth variations with  $V_{DS}$  for a fixed  $V_{GS}$ , and remains practically constant after the onset of current saturation.

With the current-operation mode it is not possible to know a-priori which is the spatial origin of the current fluctuations. Nevertheless, several models point out that the main noise contributions come from the ohmic part of the channel, i.e., the part under the gate on the side of the source [4], [20], [23]. This explains why  $S_{i_D}$  does not change with  $V_{DS}$  when the MESFET is saturated. Indeed, under these conditions that region of the device is not substantially affected by the increase of the drain voltage. Furthermore, when  $V_{GS}$  is modified, the concentration of free carriers in that part of the channel is significantly altered, and therefore the level of noise changes.

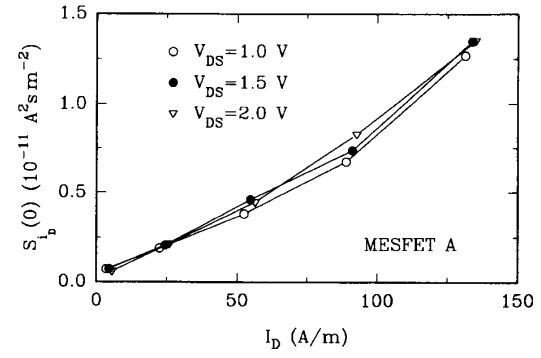


Fig. 7. Low-frequency value of the spectral density of short-circuit drain-current fluctuations as a function of the drain current for several drain voltages in the saturation region of MESFET A.

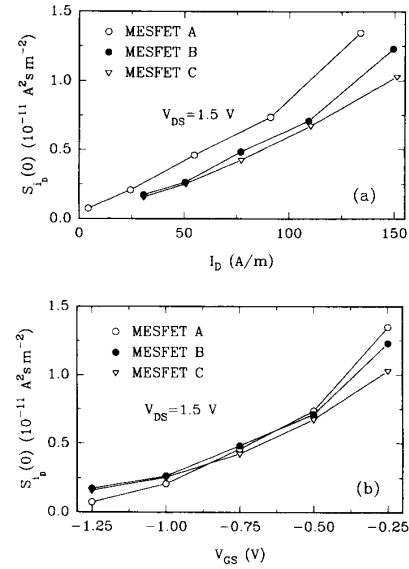


Fig. 8. Low-frequency value of the spectral density of short-circuit drain-current fluctuations for  $V_{DS} = 1.5$  V in the three MESFET geometries considered: (a) as a function of the drain current; (b) as a function of the gate voltage.

Fig. 7 reports the dependence of  $S_{i_D}$  on the drain current in the saturation region of MESFET A. The spectral density increases almost linearly with the current except for a superlinear tendency at the highest values. This behavior is exactly the same as that found numerically and experimentally in [24]. As already mentioned,  $S_{i_D}$  does not depend on the value of  $V_{DS}$ , but on the level of the current flowing through the device.

The values of  $S_{i_D}$  obtained under saturation conditions in the three MESFET geometries considered are shown in Fig. 8. The dependence on the drain current and on the gate-to-source voltage is similar in the three devices. For the same value of the drain current, the noise is lower in MESFET's B and C [Fig. 8(a)], since an important part of the current is flowing through the substrate, which is a highly-resistive region that contributes to the drain-current noise less than the  $n$  channel (through which all the current is flowing in

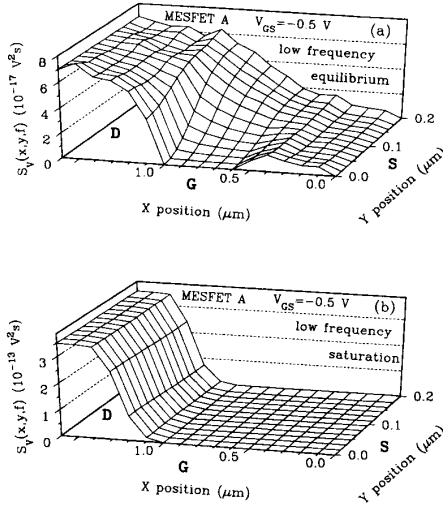


Fig. 9. Spatial map inside MESFET A of the low-frequency value of the spectral density of voltage fluctuations (with respect to the source) for two bias points: (a) equilibrium,  $V_{GS} = -0.5$  V,  $I_D = 0.0$  A/m (corresponding to an average drain voltage of 0.0 V), (b) saturation,  $V_{GS} = -0.5$  V,  $I_D = 91.1$  A/m (corresponding to an average drain voltage of 1.3 V). The positions of the source (S), the gate (G) and the drain (D) are indicated in the figure.

MESFET A). This means that the presence of the substrate, which degrades the MESFET ac behavior [19], improves the noise performance related to the drain current. This conclusion may be misleading if it is extrapolated to the noise in general, since here we are only dealing with diffusion noise. For example, the presence of deep traps in the substrate can lead to the appearance of generation-recombination noise [25]; and other noise parameters, like the minimum noise figure, are deteriorated by the lower value of the transconductance  $g_m$  in the devices with substrate [20]. In Fig. 8(a) it is also observed that  $S_{i_D}$  is always slightly lower in MESFET C, when the gate is displaced toward the source, than in MESFET B. This is related to the reduction of the ohmic part of the channel, main origin of the drain-current noise. When  $S_{i_D}$  is plotted versus  $V_{GS}$  [Fig. 8(b)], the differences found among the different MESFET's are strongly reduced, since the part of the channel depleted by the gate for a given  $V_{GS}$  is essentially the same in the three devices, and the carrier concentration in the source side of the channel is similar.

### B. Voltage-Noise Operation

Within this operation mode we shall focus on the drain-voltage fluctuations and their spatial origin. Fig. 9 shows the low-frequency value of the spectral density of voltage fluctuations (as measured from the source contact),  $S_V(x, y; f)$ , as a function of the position inside MESFET A for fixed values of  $V_{GS}$  and  $I_D$  corresponding to the conditions of equilibrium ( $V_{GS} = -0.5$  V,  $I_D = 0.0$  A/m) and saturation ( $V_{GS} = -0.5$  V,  $I_D = 91.1$  A/m). Here the spatial distribution of the voltage noise can be clearly observed. Of course, in the drain contact the value of the spectral density must be the same for all the  $y$  positions, and in the gate contact must be null since its voltage is kept constant in time.

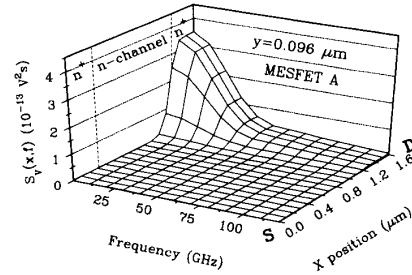


Fig. 10. Spectral density of voltage fluctuations (with respect to the source) as a function of frequency and  $x$  position for a fixed  $y$  position corresponding to  $0.096 \mu\text{m}$  in MESFET A at the operating point  $V_{GS} = -0.5$  V,  $I_D = 91.1$  A/m (average drain voltage of 1.3 V). The positions of the source (S) and the drain (D) are indicated in the figure.

In contrast with the drain-current noise, for a fixed  $V_{GS}$  the low-frequency value of the drain-voltage noise increases as the average value of  $V_{DS}$  becomes higher. Such an increase is initially smooth in the linear region of the  $I_D$ - $V_{DS}$  characteristic, and then becomes sharp when the saturation region is reached, due to the strong decrease of the output conductance  $g_{ds}$ . In Fig. 9 it can be observed that there is a difference of more than three orders of magnitude between the values of the spectral density in equilibrium and in saturation conditions. Moreover, the spatial origin of the noise is quite different in the two conditions.

At equilibrium, the presence of the constant voltage in the gate modulates the voltage spectrum in the  $y$  direction along the channel. Thus, in the regions which are far from the gate, the voltage fluctuations are found to be distributed mainly along the whole  $n$  region, while approaching the gate these are concentrated in the vicinity of the drain  $n^+$  region. In the case of saturation, the distribution of the voltage noise changes drastically. There is almost no dependence on the  $y$  position. The spatial origin of the fluctuations is localized in the zone of the  $n$  channel between the gate and the drain, and even penetrates the drain  $n^+$  region. It is due to the fact that this is the part of the device which absorbs all the variations of the drain voltage, screening their effect on the source region. Moreover, an important presence of hot carriers (and upper-valley population) takes place in this same region, which makes it highly resistive, thus increasing the voltage fluctuations. This presence of hot carriers extends into the drain  $n^+$  region, and makes the low-frequency noise penetrate inside it. This effect was already seen in  $n^+nn^+$  structures [6]. Similar results for the spatial origin of the voltage fluctuations under saturation conditions have been obtained in [26] by using the impedance-field method.

Fig. 10 shows the spectral density of voltage fluctuations along the channel in the  $y$  position corresponding to  $0.096 \mu\text{m}$  as a function of frequency and  $x$  position for MESFET A at the operating point corresponding to saturation ( $V_{GS} = -0.5$  V,  $I_D = 91.1$  A/m). Here it can be clearly observed that the increase in the drain-voltage noise takes place mainly at the lowest frequencies (between 0 and 30 GHz) and is localized between the gate and the drain; the penetration in the drain  $n^+$  region being less pronounced as the frequency increases.

The drain-voltage noise under saturation is much lower in MESFET's B and C due to the higher value of the output conductance  $g_{ds}$  in these devices. The spatial origin of the voltage fluctuations is similar to that of MESFET A.

## V. CONCLUSIONS

We have presented a two-dimensional MC analysis of electronic noise associated with carrier velocity fluctuations in GaAs MESFET's by investigating the current and voltage spectral densities at the gate and drain terminals. An accurate estimator of the currents at the contacts has been used. Three different MESFET geometries have been studied and two noise representations have been considered in the analysis. Under saturation conditions, the noise in the drain current has been found to be independent from frequency in the whole range of device operation and to increase almost linearly with the level of the current. The presence of a semi-insulating substrate and the displacement of the gate toward the source contact reduce the fluctuations in the drain current. The noise in the gate current increases quadratically with frequency up to 100 GHz. The spectral density of drain-voltage fluctuations increases with the level of the drain current, specially in the saturation region. The spatial origin of the voltage noise has been determined. Accordingly, under current saturation the voltage fluctuations are localized in the zone of the  $n$  channel between the gate and the drain, and penetrate into the drain  $n^+$  region due to the presence of carriers in the upper valleys. As final remark, the MC method, by incorporating naturally the processes responsible for the fluctuations, has been proven to be a useful tool for the analysis of noise in three-terminal devices.

## ACKNOWLEDGMENT

The authors gratefully acknowledge helpful discussions with Professor E. Velázquez of Salamanca University (Spain). This work, which has been performed within the European Laboratory for Electronic Noise (ELEN), has been partially supported by the project SA-14/14/92 from the Consejería de Cultura de la Junta de Castilla y León, and by the Commission of European Community through the contracts EKBXCT920047 and ERBCHBCT920162.

## REFERENCES

- [1] A. Cappy, "Noise modeling and measurement techniques," *IEEE Trans. Microwave Theory Technol.*, vol. 36, pp. 1–10, Jan. 1988.
- [2] K. M. van Vliet, "The transfer-impedance method for noise in field-effect transistors," *Solid-State Electron.*, vol. 22, pp. 233–236, 1979.
- [3] A. Cappy and W. Heinrich, "High-frequency FET noise performance: A new approach," *IEEE Trans. Electron Devices*, vol. 36, pp. 403–409, Feb. 1989.
- [4] G. Ghione and F. Filicori, "A computationally efficient unified approach to the numerical analysis of the sensitivity and noise of semiconductor devices," *IEEE Trans. Computer-Aided Design*, vol. 12, pp. 425–438, Mar. 1993.
- [5] J. Zimmermann and E. Constant, "Application of Monte Carlo techniques to hot carrier diffusion noise calculation in unipolar semiconductor components," *Solid-State Electron.*, vol. 23, pp. 915–925, 1980.
- [6] T. González, D. Pardo, L. Varani, and L. Reggiani, "Spatial analysis of electronic noise in submicron semiconductor structures," *Appl. Phys. Lett.*, vol. 63, pp. 84–86, 1993.
- [7] T. González, D. Pardo, L. Varani, and L. Reggiani, "Monte Carlo analysis of noise spectra in Schottky-barrier diodes," *Appl. Phys. Lett.*, vol. 63, pp. 3040–3042, 1993.
- [8] L. Varani, L. Reggiani, T. Kuhn, T. González, and D. Pardo, "Microscopic simulation of electronic noise in semiconductor materials and devices," *IEEE Trans. Electron Devices*, vol. 41, pp. 1916–1925, 1994.
- [9] A. Yoshii, M. Tomizawa, and K. Yokoyama, "Accurate modeling for submicrometer-gate Si and GaAs MESFET's using two-dimensional particle simulation," *IEEE Trans. Electron Devices*, vol. 30, pp. 1376–1380, Oct. 1983.
- [10] Y. Awano, K. Tomizawa, and N. Hashizume, "Principles of operation of short-channel Gallium Arsenide field-effect transistor determined by Monte Carlo method," *IEEE Trans. Electron Devices*, vol. 31, pp. 448–452, Apr. 1984.
- [11] S. E. Laux, M. V. Fischetti, and D. J. Frank, "Monte Carlo analysis of semiconductor devices: The DAMOCLES program," *IBM J. Res. Develop.*, vol. 34, pp. 466–494, July 1990.
- [12] C. Moglestue, "A Monte Carlo particle study of the intrinsic noise figure in GaAs MESFET's," *IEEE Trans. Electron Devices*, vol. 32, pp. 2092–2096, Oct. 1985.
- [13] M. B. Patil and U. Ravaioli, "Transient simulation of semiconductor devices using the Monte-Carlo method," *Solid-State Electron.*, vol. 34, pp. 1029–1034, 1991.
- [14] V. Gruzinskis, S. Kersulis, and A. Reklaitis, "An efficient Monte Carlo particle technique for two-dimensional transistor modeling," *Semicond. Sci. Technol.*, vol. 6, pp. 602–606, 1991.
- [15] T. González, D. Pardo, L. Varani, and L. Reggiani, "Monte Carlo simulation of electronic noise in MESFET's," in *Proc. of 1994 Gallium Arsenide Applications Symposium (GAAS 94)*, Torino, Italy, Apr. 1994, pp. 385–388.
- [16] C. Jacoboni and P. Lugli, *The Monte Carlo Method for Semiconductor Device Simulation*. Vienna: Springer-Verlag, 1989.
- [17] T. González, J. E. Velázquez, P. M. Gutiérrez, and D. Pardo, "Five-valley model for the study of electron transport properties at very high electric fields in GaAs," *Semicond. Sci. Technol.*, vol. 6, pp. 862–871, 1991.
- [18] H. Rothe and W. Dahlke, "Theory of noisy fourpoles," in *Proc. IRE*, vol. 44, pp. 811–818, June 1956.
- [19] T. González and D. Pardo, "Monte Carlo determination of the intrinsic small-signal equivalent circuit of MESFET's," *IEEE Trans. Electron Devices*, vol. 42, pp. 605–611, Apr. 1995.
- [20] R. A. Pucel, H. A. Haus, and H. Statz, "Signal and noise properties of gallium arsenide microwave field-effect transistors," in *Adv. Electron. Electron Phys.*, vol. 38, pp. 195–265, 1975.
- [21] A. van der Ziel, *Noise in Solid State Devices and Circuits*. New York: Wiley, 1986.
- [22] K. Y. Lee, H. S. Min, and Y. J. Park, "Estimation of noise power spectral densities from the Monte-Carlo simulated terminal currents in semiconductor devices," *Solid-State Electron.*, vol. 36, pp. 1563–1570, 1993.
- [23] J. Zimmermann and A. Cappy, "Hot electron noise in III-V heterojunction field effect transistors," *Semicond. Sci. Technol.*, vol. 7, pp. B468–B473, 1992.
- [24] G. Ghione, F. Bonani, and M. Pirola, "High-field diffusivity and noise spectra in GaAs MESFET's," *J. Phys. D: Appl. Phys.*, vol. 27, pp. 365–375, 1994.
- [25] Z.-M. Li, S. P. McAlister, and D. J. Day, "Analytical model of low-frequency diffusion noise in GaAs MESFET's," *IEEE Trans. Electron Devices*, vol. 38, pp. 232–236, Feb. 1991.
- [26] A. Abou-Elnour and K. Schuenemann, "Two-dimensional noise calculations of sub-micrometer MESFET's," in *Proc. ESSDERC 92, Microelectron. Eng.*, vol. 19, pp. 43–46, 1992.

**Tomás González**, for a photograph and biography, see p. 611 of the April 1995 issue of this TRANSACTIONS.

**Daniel Pardo**, for a photograph and biography, see p. 611 of the April 1995 issue of this TRANSACTIONS.



**Luca Varani** was born in Carpi, Italy, in 1963. He received the diploma degree in physics in 1989 and the Ph.D. degree in physics in 1993 from Modena University, Italy.

He is currently working at the Centre d'Electronique de Montpellier, Montpellier, France, in the Human Capital and Mobility Program. His main research activity is in the field of electronic transport in semiconductors with special application to Monte Carlo simulation of electronic noise. He is the author or coauthor of about 60 scientific papers.

Dr. Varani is a member of the Italian and the European Physical Societies.



**Lino Reggiani** was born in Modena, Italy, in 1941. He received the Dr. in Physics degree in 1968 and the Diploma di Perfezionamento in physics in 1972 from Modena University.

From 1972 to 1982, he was an Assistant Professor and later Associate Professor in the Physics Department of Modena University. He has been the Director of the Computer Center at Modena University since 1990. His main research activity has been in the field of electronic transport in semiconductors, including Monte Carlo simulation of noise. He has authored or coauthored approximately 160 scientific works, and is the editor of *Hot-Electron Transport in Semiconductors* (Springer-Verlag, 1985).

Dr. Reggiani is a member of the Italian Physical Society.